American Mineralogist, Volume 72, pages 1071–1085, 1987

Solubility of carbon dioxide in albitic melt

EDWARD STOLPER, GERALD FINE,[1] THOMAS JOHNSON,[2] SALLY NEWMAN
Division of Geological and Planetary Sciences, California Institute of Technology, Pasadena, California 91125, U.S.A.

ABSTRACT

Infrared spectroscopy has been used to measure the concentrations of molecular CO_2 and carbonate in albitic ($NaAlSi_3O_8$) glasses quenched from melts equilibrated with CO_2 vapor at high pressures (15–30 kbar) and temperatures (1450–1625 °C). At constant temperature, the concentrations of carbonate and molecular CO_2 as well as the CO_3^{2-}/CO_2 ratio increase with increasing pressure under vapor-saturated conditions. The second derivative of these species concentrations with respect to pressure under vapor-saturated conditions at constant temperature is positive over the range of conditions studied. At constant pressure under vapor-saturated conditions, the solubility of molecular CO_2 decreases with increasing temperature, but the concentration of carbonate increases. The net effect is that total CO_2 solubility is nearly independent of temperature. According to our results, CO_2 solubility and speciation change gradually over the range of conditions that we have studied and do not indicate major or abrupt structural changes in albitic melts in this *P-T* range.

Our results can be described thermodynamically in terms of two reactions. The first, CO_2(vapor) = CO_2,molecular(melt), describes the heterogeneous equilibrium between melt and vapor. The second, CO_2,molecular(melt) + O^{2-}(melt) = CO_3^{2-}(melt), models the homogeneous equilibrium between melt species. Volume and enthalpy changes of these two reactions have been constrained by our solubility and speciation data. We emphasize that the solubilities of volatile components that dissolve in melts in several different forms must be treated by such coupled heterogeneous and homogeneous equilibria and that spectroscopic methods provide direct insights into them.

INTRODUCTION

The solubility of CO_2 in both natural and synthetic silicate melts has been studied extensively in recent years. There have been several motivations for these studies. First, solubility measurements give upper limits on the amounts of CO_2 that can dissolve in magmas at various temperatures and pressures. Such data are essential if we are ever to understand the degassing behaviors of magmas as they ascend (e.g., Moore, 1979; Spera and Bergman, 1980; Mathez, 1984). Moreover, information on the pressure and temperature dependence of CO_2 solubility and spectroscopic studies of quenched CO_2-saturated melts may provide insights into the mechanisms of CO_2 dissolution (e.g., Mysen, 1976; Rai et al., 1983) and into the structures and properties of silicate melts (e.g., Mysen, 1976, 1977).

It is known that CO_2 dissolves in silicate melts in at least two microscopic forms: molecules of CO_2 and carbonate ion complexes (Mysen, 1976; Fine and Stolper, 1985, 1986). CO_2 solubility (i.e., the concentration of CO_2 in a melt in equilibrium with CO_2 vapor) is the sum of the concentrations of the various forms of dissolved CO_2. Full understanding of the effects of pressure, temperature, and silicate composition on the solubility of CO_2 in melts must therefore take account both of the heterogeneous equilibrium between melt and vapor and of the homogeneous equilibria between various melt species. Measurements of the concentrations of the different forms of dissolved CO_2 in vapor-saturated melts thus have the potential to provide greater insights into the thermodynamics of solubility and into the microscopic mechanisms that contribute to observed variations in solubility than do simple measurements of bulk dissolved CO_2 contents that give no direct information on speciation.

In this paper, we report new measurements of the solubility of CO_2 in albitic melt at pressures of 15–30 kbar and temperatures of 1450–1625 °C. Bulk CO_2 concentrations were determined by summing the concentrations of dissolved carbonate ions and molecules of CO_2 in glasses quenched from melts equilibrated with CO_2-rich vapor at high temperatures and pressures. The concentrations of the individual C-bearing species in the glasses were determined by infrared spectroscopy, in which the intensities of absorptions due to the presence of these species were measured. The albitic composition was chosen be-

[1] Present address: Research and Development Division, Corning Glass Works, Corning, New York 14831, U.S.A.

[2] Present address: Department of Geology and Geophysics, University of California, Berkeley, California 94720, U.S.A.

0003–004X/87/1112–1071$02.00

TABLE 1. Average of five microprobe analyses of the albitic glass used in this study

	Analyzed	Ideal
Na_2O	10.38	11.82
Al_2O_3	20.43	19.44
SiO_2	69.66	68.74
Total	100.47	100.00

Note: Microprobe conditions were acclerating voltage, 15 kV; sample current, 5 nA on brass; beam size, 40–50 μm. Also given is an analysis of stoichiometric albite.

cause it is a traditional and simple starting point for modeling real magmatic systems, because previous measurements of solubility and speciation are available in the literature for comparison (Brey, 1976; Mysen, 1976; Mysen et al., 1976; Mysen and Virgo, 1980), and because we have previously calibrated the infrared technique for quantitative determination of the concentrations of C-bearing species in albitic glass (Fine and Stolper, 1985).

Experimental techniques

The synthesis of CO_2-bearing glass samples is discussed in detail elsewhere (Fine and Stopler, 1985, 1986), but is reiterated briefly here. Starting material of approximately albite ($NaAlSi_3O_8$) composition was synthesized by grinding Johnson-Matthey Specpure Na_2CO_3, Al_2O_3, and SiO_2 in an agate mortar for 6 h, followed by melting at 1580 °C for 12 h in air at 1 atm. This decarbonated glass was ground under ethanol for 6 h and dried at 850 °C in air for 2 d to remove adsorbed water and hydrocarbon residue. An electron-microprobe analysis of the decarbonated glass is given in Table 1. Although microprobe analyses of soda-rich glasses are difficult because of Na mobility under the electron beam, the glass appears to be deficient in Na_2O relative to stoichiometric albite, probably owing to Na volatilization during decarbonation and drying. The compostion that we studied is consequently slightly peraluminous (3.4% normative corundum) and enriched in silica relative to stoichiometric albite.

Powdered silicate starting material and silver oxalate ($Ag_2C_2O_4$) were weighed into Pt capsules that were then sealed by arc-welding. Amounts of each were chosen using published solubility data to produce vapor-saturated melts with a minimum of excess vapor. These Pt capsules were in turn loaded into larger Pt capsules containing sintered hematite and run in a 0.5-in. (1.27-cm) piston-cylinder apparatus using an NaCl and Pyrex pressure medium at a variety of pressures (15–30 kbar) and temperatures (1450–1625 °C) using the procedures described in Fine and Stolper (1985).

During run conditions, the silver oxalate presumably dissociates to Ag metal and CO_2. Upon quenching, glasses containing disseminated Ag and dissolved CO_2 are formed. No quench crystalline carbonates were observed. The glasses are often yellow or bluish-orange, probably owing to finely disseminated Ag (Seward, 1980). All of the glasses contain bubbles from 5 to 100 μm in diameter that are assumed to contain gaseous or liquid CO_2; the bubbles tend to occur in streaks and clusters distributed throughout the sample. We have interpreted the presence of these bubbles as an indication of vapor-saturated conditions during the experiments.

A few vapor-saturated and undersaturated CO_2-bearing glasses were prepared for us by A. L. Boettcher of the University of California. These samples were prepared in a 1-in. (2.54-cm) piston-cylinder apparatus using dried crystalline albite plus silver oxalate as starting materials.

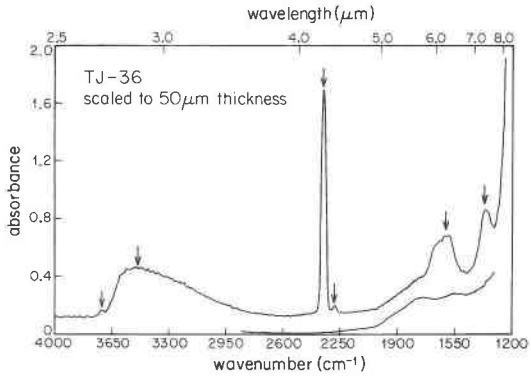

Fig. 1. Spectrum of a CO_2-bearing albite glass (TJ-36) scaled to a thickness of 50 μm. The six absorption bands discussed in the text are indicated by arrows. The lower spectrum is of a CO_2-free albite glass (ABC-12: 1400 °C, 20 kbar, 0.19 wt% H_2O) scaled to the same thickness.

A few albitic and jadeitic glasses were synthesized at pressures of 100 to 1000 bars at 1200 °C in an internally heated Ar pressure vessel in J. R. Holloway's laboratory at the Arizona State University. These samples were uniformly charged with bubbles up to 20 μm in size.

The quenched glasses were sectioned with a diamond saw, ground into plates 30–250 μm in thickness, and polished on both sides in a slurry of Al_2O_3 and H_2O. Sample thickness was measured with a digital dial indicator. The polished glass plates were placed over metal apertures 50–1000 μm in diameter. The samples were then examined microscopically to determine whether bubbles were present in the region exposed by the aperture. In most cases, spectra were obtained on bubble-free or nearly bubble-free regions. In some cases, however, bubble-rich regions were purposely examined so that we could examine the spectroscopic signature of CO_2 contained in bubbles.

Transmission infrared spectra were obtained on the regions of the samples exposed by the metal aperture using both a Perkin-Elmer 180 infrared spectrophotometer and a Nicolet Instruments 60SX Fourier transform infrared spectrometer (FTIR). These machines yielded quantitatively similar results, but the FTIR is quicker and has the advantage of smaller potential beam sizes (less than tens of micrometers). Infrared spectra on the FTIR were obtained using a $HgCdTe_2$ detector, KBr beamsplitter, globar source, a mirror velocity of 1.57 cm/s, and 1024 to 8192 scans.

Infrared spectroscopy of CO_2-bearing glasses

Band assignments

Typical spectra of a CO_2-bearing and a CO_2-free albitic glass are shown in Figure 1. Six absorption bands are present in the CO_2-bearing glass that are not observed in the CO_2-free glass.

2352 cm^{-1}. This sharp, intense band is due to the ν_3 antisymmetric stretching mode of $^{12}CO_2$ molecules dissolved in the glass (Fine and Stolper, 1985). The band is slightly asymmetrical; it can be approximated as the sum

of two nearly Gaussian bands, one at about 2350 cm^{-1} (FWHM = full width at half maximum = 19 cm^{-1}) and a second band at about 2370 cm^{-1} (FWHM = 15 cm^{-1}) with about 15% of the intensity of the first band. The position and shape of the band in bubble-free glasses change little between room temperature and liquid-nitrogen temperature. This contrasts with the spectra of bubble-rich samples, which at room temperature have an absorption maximum at about 2358–2366 cm^{-1}, sometimes with a shoulder at 2340–2350 cm^{-1}, and often showing a conspicuous dip in the baseline of the spectrum centered at about 2310 cm^{-1}. At liquid-nitrogen temperature, the band at ~2360 cm^{-1} is split into three sharp peaks at 2337, 2352, and 2366 cm^{-1} plus a sharp peak at 2281 cm^{-1}, and the anomalous baseline in this region of the spectrum is no longer present. We presume that this spectrum is characteristic of crystalline CO_2 within the bubbles at low temperatures.

2287 cm^{-1}. This weak band on the sloping tail of the band at 2352 cm^{-1} is attributed to the ν_3 antisymmetric stretch of dissolved molecules of $^{13}CO_2$ (Fine and Stolper, 1985). No attempt has been made to model its shape, but its FWHM is approximately 20 cm^{-1} and changes little between room temperature and liquid-nitrogen temperature, though the background is flatter under these conditions because of a narrowing of the band at 2352 cm^{-1} in this vicinity.

For bubble-rich samples at room temperature, this band is usually a poorly defined shoulder on the $^{12}CO_2$ band at 2352 cm^{-1}, and it is often difficult to see because of the distortion of the baseline of very bubble-rich glasses described above. It is sometimes resolvable into two weak bands in bubble-rich samples: one at 2310 cm^{-1} and a second at 2275 cm^{-1}. These two bands may be the $^{13}CO_2$ equivalents of the $^{12}CO_2$ bands observed at ~2360 cm^{-1} and ~2345 cm^{-1} in bubble-rich samples. In bubble-rich samples at liquid-nitrogen temperatures, however, the broad bands in this region are replaced by a distinct band at 2281 cm^{-1}. In samples containing significant CO_2 both in bubbles and in the enclosing glass, the spectrum again shows a broad shoulder in this region at room temperature, which resolves into bands at about 2290 and 2284 cm^{-1} at liquid-nitrogen temperature. The band at higher wave numbers is assigned to dissolved molecules of $^{13}CO_2$ and the one at lower wave numbers to frozen $^{13}CO_2$ in the bubbles.

3710 cm^{-1}. This weak band is due to the presence of molecules of CO_2, as indicated by its strength in bubble-rich samples synthesized at low pressures and the excellent ($r = 0.98$) correlation of its intensity with the $^{13}CO_2$ band at 2287 cm^{-1} in bubble-free glasses. We tentatively assign this band to a combination of the ν_1 and ν_3 modes of $^{12}CO_2$ molecules (Nakamoto, 1978; Fine and Stolper, 1985). In bubble-free specimens, the band shape changes very little between room temperature and liquid-nitrogen temperature; in bubble-rich specimens, the band sharpens considerably at liquid-nitrogen temperature.

3550 cm^{-1}. This broad, asymmetric band is attributed to the stretching of OH groups and water molecules dissolved in the glass (Stolper, 1982a). It appears to be difficult to completely exclude water from glasses synthesized at elevated pressures and temperatures in solid media piston-cylinder apparatuses (Fine and Stolper, 1985). This is particularly true in CO_2-bearing experiments, which systematically have higher water contents than glasses synthesized without CO_2.

1600–1700 cm^{-1} and 1375 cm^{-1}. These bands are attributed to CO_2 dissolved in the form of distorted CO_3^{2-} ionic complexes (Fine and Stolper, 1985). The shapes of these bands change little between room and liquid nitrogen temperatures. The band between 1600 and 1700 cm^{-1} is clearly a composite; we have found that it can be approximated as a sum of two nearly Gaussian components, one at 1670–1680 cm^{-1} (FWHM = 70–80 cm^{-1}) and another at 1600–1610 cm^{-1} (FWHM = 70–80 cm^{-1}). The relative intensities of these two components are variable, but are usually within about 20% of each other for the albitic glasses reported on in this paper. The same two components are present in CO_2-bearing jadeitic glasses, but the component at 1600–1610 cm^{-1} is typically about 50–80% larger than the one at 1670–1680 cm^{-1}. This is apparent in the spectra presented in Fine and Stolper (1985). In both albitic and jadeitic glasses, the band at 1375 cm^{-1} can be approximated by a single Gaussian component (FWHM = ~70 cm^{-1}). Following our earlier interpretation (Fine and Stolper, 1985, and references therein), these bands, including the component at 1670–1680 cm^{-1}, are interpreted as splittings of the ν_3 stretching vibrations of distorted sodium carbonate ionic complexes. We do not have specific assignments or interpretations of the observed spectral components in terms of the local structural details of the dissolved carbonate ionic complexes responsible for them, but similar spectral features observed in nitrate glasses have been analyzed in some detail (Furukawa et al., 1978).

At elevated water contents, we would expect to observe an absorption at 1630 cm^{-1} due to molecular H_2O. We have not observed such a component in the spectra of the glasses included in this study, nor have we observed a correlation between total water content and the ratio of the integrated intensities of the 1600–1700-cm^{-1} and 1375-cm^{-1} bands that we would expect to accompany such a component. On the basis of the total water contents of our CO_2-saturated glasses, the observed relationship between total water and molecular H_2O contents of albitic glasses, and the molar absorptivity of the 1630 cm^{-1} band in albitic glasses (L. A. Silver and E. Stolper, in prep.), the intensity of the 1630-cm^{-1} molecular H_2O band would be expected in all cases to be less than 10% of the intensity of the carbonate bands at 1600–1700 cm^{-1}.

Band intensities

Quantitative measurements of band intensities were made of most of the absorption bands on each of the glass samples. These measurements were made on each spectrum after the spectrum of a CO_2-free albite glass, scaled

TABLE 2. Molar absorptivities and integrated molar absorptivities for relevant infrared absorption bands in albitic glass

Band (cm^{-1})	Species	ϵ (L/mol·cm)	ϵ^* (L/mol·cm^2)
3710	molecular CO_2	13.9 ± 1.1	485 ± 40
3550[A]	OH, H_2O	70 ± 2	35 000 ± 500
2350	molecular $^{12}CO_2$	945 ± 45	25 200 ± 1 200
2287	molecular $^{13}CO_2$	11.7 ± 1.0[B]	—
1610[C]	carbonate	199 ± 17	27 300 ± 2 300
1375	carbonate	235 ± 20	16 300 ± 1 400

Note: Values determined as described in the text. Errors for ϵ_{2350} and ϵ_{1375} evaluated as described in Fine and Stolper (1985). All others based on propagation of these errors with the standard errors obtained by regression of band intensities against the 2350-cm^{-1} or 1375-cm^{-1} band intensities; i.e., the best-fit ratio of intensities of the 2350- and 3710-cm^{-1} bands is 68 with a standard error of 4, so $\epsilon_{3710} = \epsilon_{2350}/68 = 13.9$, and the error on ϵ_{3710} is $13.9 \times [(4/68)^2 + (45/945)^2]^{1/2}$.

Species concentrations (as weight percent of CO_2 that would be released from the sample if all of the species were converted to CO_2 and removed) can be calculated as follows: c = (absorbance × 44.01)/(density × thickness × ϵ), where density is in g/L and thickness is in cm. If integrated absorbance is used, ϵ is replaced with ϵ^*. For water contents, 44.01 is replaced by 18.02.

[A] From Silver and Stolper (in prep.).

[B] This value has been refined since our preliminary report of this work (Johnson et al., 1985). The concentrations listed in Table 3 are based on the extinction coefficients given here and superceded previously reported values.

[C] This refers to the maximum peak height or total integrated intensity of the group of bands between 1600 and 1700 cm^{-1}.

to the thickness of the CO_2-bearing glass, had been numerically subtracted from it. This resulted in a spectrum with a relatively flat background from which the peak heights and areas of the bands at 3550, 2350, 1600–1700, and 1375 cm^{-1} could be readily determined. The band at 3710 cm^{-1} sits on the high-energy tail of the band at 3550 cm^{-1}; its intensity and integrated intensity were determined after the 3550 cm^{-1} band had been approximately nulled out by numerical subtraction of the spectrum of a water-bearing, CO_2-free albitic glass. The 2287-cm^{-1} band due to $^{13}CO_2$ sits on the low-energy tail of the $^{12}CO_2$ band at 2352 cm^{-1}. Unfortunately, we do not have spectra of $^{12}CO_2$-bearing glasses that contain no $^{13}CO_2$, so the shape of the low-energy tail of the $^{12}CO_2$ band on which the $^{13}CO_2$ band sits is not unambiguously known. Consequently backgrounds for this band were drawn by hand.

Although intensities of all six of the absorption bands could, in principle, be measured from each spectrum, in practice, there are several limitations. The first is that absorbances greater than 1.5–2.0 cannot be reliably measured on our instruments. Hence, for very intense absorptions, intensities cannot be determined precisely. This is usually the case for the $^{12}CO_2$ band at 2352 cm^{-1}; samples would have to be unrealistically thin (i.e., less than a few tens of micrometers) in order for this absorption to be on scale for the concentrations of molecular CO_2 in most of the vapor-saturated glasses that we synthesized. Consequently, the bands at 3710 and 2287 cm^{-1} were used nearly exclusively in this study for determining molecular CO_2 concentrations. In the case of the carbonate bands, these sit on the high-energy tail of the prominent aluminosilicate bands in the mid-infrared. If the samples are thicker than 200 μm or so, the background can be so intense that the carbonate absorptions are off scale. Thin samples (<100 μm) can also present problems because interference fringes are sometimes present in the spectra of such specimens and these limit the accuracy with which absorption intensities can be measured, particularly for weak absorptions.

Determination of extinction coefficients

In order to determine the concentration in the glass of the species responsible for a particular absorption, we must know the band intensity, the sample thickness, the glass density (estimated in this study from the data of Kushiro, 1978, on CO_2-free albitic glasses quenched from melts at temperatures and pressures similar to those of our study), and the extinction coefficient (or molar absorptivity) of the band in question. The extinction coefficient is the constant of proportionality between the intensity of the absorption and the number of absorbers per unit area in the path of the infrared beam. It must be determined empirically by determining the intensity of the absorption band in samples in which the concentration of the absorber is known. Molar absorptivities and integrated molar absorptivities have been previously determined for the molecular $^{12}CO_2$ band at 2352 cm^{-1} and for the carbonate bands at 1600–1700 and 1375 cm^{-1} by Fine and Stolper (1985) using a series of synthetic CO_2-bearing glasses near the jadeite-silica join. Details of the procedure used to determine these coefficients and of its uncertainties are given in that paper. The values of these constants used in this paper are listed in Table 2; the integrated molar absorptivities for the carbonate bands, which were determined as in Fine and Stolper (1985) by the best-fit ratio of the integrated band intensity to the peak height for each band, are slightly different from those given in Fine and Stolper (1985) since we have enlarged the data set used in determining this ratio by including the data obtained in this study. The best-fit value of the ratio of the intensities of the 1375- and 1600–1700-cm^{-1} carbonate bands has also been updated by the data obtained in this study.

The molar absorptivity for the 3710-cm^{-1} band listed in Table 2 was determined by regressing the intensity of this band with that of the 2352-cm^{-1} band for seven undersaturated albitic and jadeitic CO_2-bearing glasses from the study of Fine and Stolper (1985). Unfortunately, when the 2352-cm^{-1} band is on scale, the 3710-cm^{-1} band is very weak, and this ratio could be more tightly constrained. The integrated molar absorptivity of the 3710-cm^{-1} band and the molar absorptivity of the 2287-cm^{-1} $^{13}CO_2$ band were determined by regressing the integrated intensity of the 3710-cm^{-1} band and the peak height of the 2287-cm^{-1} band against the intensity of the 3710-cm^{-1} band. Note that the extinction coefficient of the 2287-cm^{-1} band is used to give the total dissolved molecular CO_2, not just the dissolved molecular $^{13}CO_2$, and thus can only be used when the $^{13}C/^{12}C$ ratio is normal. We also

note that the ratio of the band at 2352 cm^{-1} due to molecular $^{12}CO_2$ to the band at 2287 cm^{-1} due to molecular $^{13}CO_2$ is, according to our preferred value, 80 ± 5, which is similar to their abundance ratio of 89; though there is no a priori reason that these ratios should be identical, it is encouraging that they are similar.

Accuracy and precision

Figure 2 compares the "actual" concentration of CO_2 (based on the amount of CO_2 included in the syntheses of these standard glasses) with the concentration of CO_2 obtained by summing the concentrations of dissolved carbonate and molecular CO_2 in the set of glasses used by Fine and Stolper (1985) to determine the molar absorptivities of the bands at 2352, 1600–1700, and 1375 cm^{-1}. The close correspondence between these two values demonstrates the feasibility of determining total dissolved CO_2 concentrations in glasses along the jadeite-silica join using infrared spectroscopy.

In a few cases, Fine and Stolper (1985) noted significant deviations between the amounts of CO_2 loaded into experiments and the concentration of dissolved CO_2 determined spectroscopically in quenched glasses recovered after the experiments. The measured concentration was in every case lower than the amount loaded into the experiment. Using the finer spatial resolution possible with the Nicolet FTIR, we have explored possible causes of these deviations. Figure 3 demonstrates that a typical undersaturated CO_2-bearing glass of the sort used in the calibration procedure is zoned, with higher dissolved CO_2 and lower H_2O contents in the core of the sample than in the rim next to the enclosing Pt capsule. Though other explanations are possible, we suggest that this is due to diffusion of H into the Pt capsule followed by reaction of the H with dissolved CO_2 to form some H_2O and reduced C species. The reduced C species either then remains in situ or diffuses as atomic C out of the Pt capsule as suggested by Watson et al. (1982). This can account for the systematically higher dissolved water contents of glasses synthesized with CO_2 over those without CO_2, the positive correlation between run length and dissolved water content and its negative correlation with dissolved CO_2 content that has been observed for undersaturated glasses (see Table 3 for the results of experiments conducted by A. L. Boettcher), and the fact that undersaturated glasses occasionally contain significantly less CO_2 than was loaded into the capsule prior to synthesis. As shown in Figure 3, however, the concentration measured in the center of the capsule by infrared spectroscopy is essentially identical to the amount loaded into the capsule, giving us added confidence in the accuracy of our primary calibration.

The precision of the infrared determinations of species concentrations is difficult to assess in general. Under optimum circumstances, the precision will be on the order of a few percent based on potential uncertainties in measured absorbances (typically 0.005 for an absorbance of 0.1 with the FTIR based on the reproducibility of individual measurements), in estimated density (±2%), and sample thickness (±3 μm) and varies from sample to sample. However, as discussed above, a number of factors (interference fringes in thin samples, ambiguities in background subtractions, nonlinearity of absorbances for very intense absorptions) may degrade the precision for any individual measurement. On the basis of repeated measurements of identical spots on several samples and multiple measurements of individual species concentrations on a single spot (e.g., we could make six potential measurements of molecular CO_2 concentration from any spectrum: peak heights and integrated intensities of the bands at 3710, 2352, 2287 cm^{-1}), typical uncertainties (1σ) for the samples reported on in this study are on the order of 0.1 wt% or better for dissolved molecular CO_2, 0.02 wt% for CO_2 dissolved as carbonate, and 0.01 wt% for dissolved water. The poorer precision of the molecular CO_2 determinations is due to the low intensities of the 3710- and 2287-cm^{-1} bands used in nearly every sample reported on in this study to determine molecular CO_2 concentrations. If thicker samples, much thinner samples (bringing the 2352-cm^{-1} band on scale), or ^{13}C-enriched CO_2 were used (increasing the intensity of the 2287-cm^{-1} band), the precision of the molecular CO_2 concentrations could be improved considerably, and we recommend that efforts be made in future studies to do one or more of these things.

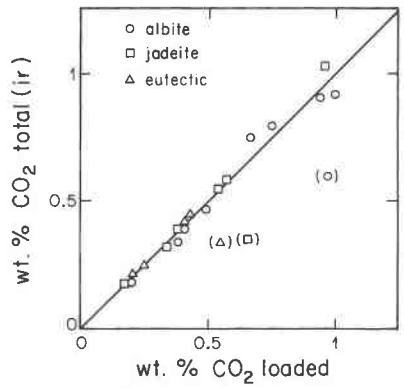

Fig. 2. Comparison of total CO_2 contents of undersaturated sodium aluminosilicate glasses synthesized by Fine and Stolper (1985) based on (1) the amount loaded into the capsule and (2) infrared spectra using the extinction coefficients given in Table 2. This figure has been updated from the work of Fine and Stolper (1985) by re-analyzing samples with the FTIR and in particular by analyzing the central portions of the samples when possible. The three symbols in parentheses show samples that appear to have lost significant CO_2 during synthesis; it is likely that these samples came from near the capsule wall. These three samples were not used in the determination of extinction coefficients.

Results

The conditions of the experiments and the measured H_2O, molecular CO_2, carbonate, and total dissolved CO_2 contents of the quenched glasses are listed in Table 3. The pressure and temperature dependence of the molec-

TABLE 3. Summary of experimental results

Run	Starting material[A]	T (°C)	Duration (min)	Wt% CO_2 loaded	H_2O[B] (wt%)	Molecular CO_2[B] (wt%)	CO_3^{2-}[B,C] (wt%)	Total CO_2[D] (wt%)
					15 kbar			
TJ41	Ab(C)	1450	65	1.9	0.61 (12, 12, 0.03)	0.59 (3, 5, 0.04)	0.18 (9, 34, 0.02)	0.77 (0.04)
ALB2965	xtal	1450	120	5	0.14 (2, 2, 0.03)	0.70[H] (2, 1, —)	0.16 (1, 2, 0.01)	0.86 (0.01)
ALB2998	xtal	1450	180	1	0.33 (1, 1, —)	0.60[H] (1, 1, —)	—[E]	—[E]
TJ42	Ab(C)	1525	60	2.4	0.72 (4, 4, 0.01)	0.55 (3, 4, 0.03)	0.21 (3, 9, 0.02)	0.76 (0.04)
					20 kbar			
TJ37	Ab(C)	1450	60	2.3	0.65 (1, 1, —)	1.12 (1, 1, —)	0.27 (1, 2, 0.01)	1.39
TJ48	Ab(C)	1450	60	—[F]	0.14 (1, 2, 0.01)	0.99 (3, 5, 0.09)	0.27 (3, 9, 0.01)	1.26 (0.10)
ALB2995[G]	xtal	1450	60	1	0.20 (3, 3, 0.07)	0.72 (3, 5, 0.03)	0.20 (3, 8, 0.01)	0.92 (0.03)
ALB2982[G]	xtal	1450	180	1	0.34 (3, 3, 0.01)	0.58 (1, 3, 0.09)	0.18 (1, 2, 0.01)	0.76 (0.10)
ALB2990[G]	xtal	1450	360	1	0.49 (1, 1, —)	0.39 (1, 1, —)	0.14 (1, 3, 0.01)	0.53
TJ4	Ab(A)	1525	100	2.4	0.42 (5, 5, 0.01)	0.95 (5, 13, 0.06)	0.28 (3, 10, 0.01)	1.23 (0.06)
TJ5	Ab(A)	1625	60	2.9	0.28 (3, 3, 0.00)	0.80 (3, 5, 0.03)	0.31 (3, 10, 0.02)	1.11 (0.04)
					25 kbar			
TJ12	Ab(A)	1450	60	2.0	0.34 (2, 2, 0.01)	1.26 (4, 10, 0.07)	0.39 (3, 10, 0.01)	1.65 (0.07)
TJ15	Ab(A)	1525	65	2.2	0.44 (4, 4, 0.02)	1.08 (2, 4, 0.12)	0.42 (4, 12, 0.01)	1.50 (0.12)
TJ22	Ab(C)	1625	60	2.0	0.42 (1, 1, —)	1.13 (1, 3, 0.05)	—[E]	—[E]
TJ36	Ab(C)	1625	60	2.2	0.56 (6, 6, 0.03)	1.05 (6, 14, 0.13)	0.47 (6, 22, 0.02)	1.52 (0.13)
					30 kbar			
TJ32	Ab(C)	1450	60	2.6	0.67 (1, 1, —)	1.44 (1, 3, 0.04)	0.50[H] (1, 1, —)	1.94
TJ33	Ab(C)	1450	65	2.7	0.69 (1, 1, —)	1.35 (1, 3, 0.07)	0.46 (1, 1, —)	1.81
TJ43	Ab(C)	1450	60	3.4	0.54 (4, 4, 0.02)	1.42 (4, 8, 0.11)	0.54 (2, 6, 0.03)	1.96 (0.11)
TJ40	Ab(C)	1525	90	3.0	0.76 (2, 2, 0.07)	1.28 (2, 4, 0.05)	0.72[H] (2, 6, 0.03)	2.00 (0.06)
TJ39	Ab(C)	1625	70	3.0	0.67 (3, 3, 0.04)	1.21 (2, 3, 0.05)	0.63 (4, 9, 0.06)	1.84 (0.08)

[A] Two separate batches of albitic glass starting material [Ab(A) and Ab(C)] were used. The ALB samples were prepared from crystalline (xtal) albite.

[B] c (n_1, n_2, σ): c is the average concentration in weight percent; n_1 is the number of separate spots or fragments for which spectra were obtained; n_2 is the number of measurements of concentration determined for this sample. $n_2 \geq n_1$ since several measurements of species concentration can usually be obtained from one spectrum. σ is the error of the reported concentration (the mean of the n_2 separate measures of concentration) given by 1σ of the distribution of the n_2 measurements.

[C] This is the amount of CO_2 dissolved as carbonate.

[D] c (σ): c is the sum of the amount of CO_2 dissolved as molecular CO_2 and as carbonate. σ is the error in this concentration based on the 1σ errors in the two species' concentrations.

[E] Concentration not determined.

[F] Not known, but the sample contains excess vapor in bubbles.

[G] These three samples were loaded with the same amount of CO_2 (1 wt%) and held at run conditions for different lengths of time. Note the decreasing CO_2 and increasing H_2O content with time. ALB2982 and 2990 do not have bubbles. Bubbles ($\lesssim$10 μm) are present but uncommon in ALB2995.

[H] These values are based on spectra of less than optimal quality.

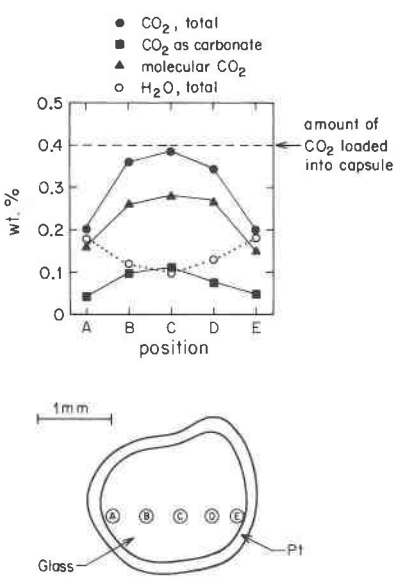

Fig. 3. Concentration profiles for dissolved CO_3^{2-}, molecular CO_2, total CO_2, and water in sample ABC-58 (Fine and Stolper, 1985). A map showing the approximate location of each measurement is also shown. The glass used is a horizontal section of a piston-cylinder run. Each analyzed spot is 100 μm in diameter. Note that the total CO_2 concentration at the capsule's center is very similar to the amount loaded into the capsule.

ular CO_2 content, carbonate content, and total dissolved CO_2 content are displayed in Figures 4 and 5.

The effects of pressure. Molecular CO_2 and carbonate concentrations, and consequently total CO_2 content, increase with increasing pressure at constant temperature. The ratio of carbonate to molecular CO_2 also increases under vapor-saturated conditions with increasing pressure at constant temperature.

The effects of temperature. The concentration of molecular CO_2 under vapor-saturated conditions decreases with increasing temperature at constant pressure, but the concentration of carbonate increases slightly. These two effects counterbalance each other, leading to a total CO_2 solubility that is nearly independent of temperature under isobaric conditions. The ratio of carbonate to molecular CO_2 increases with increasing temperature under vapor-saturated conditions at constant pressure.

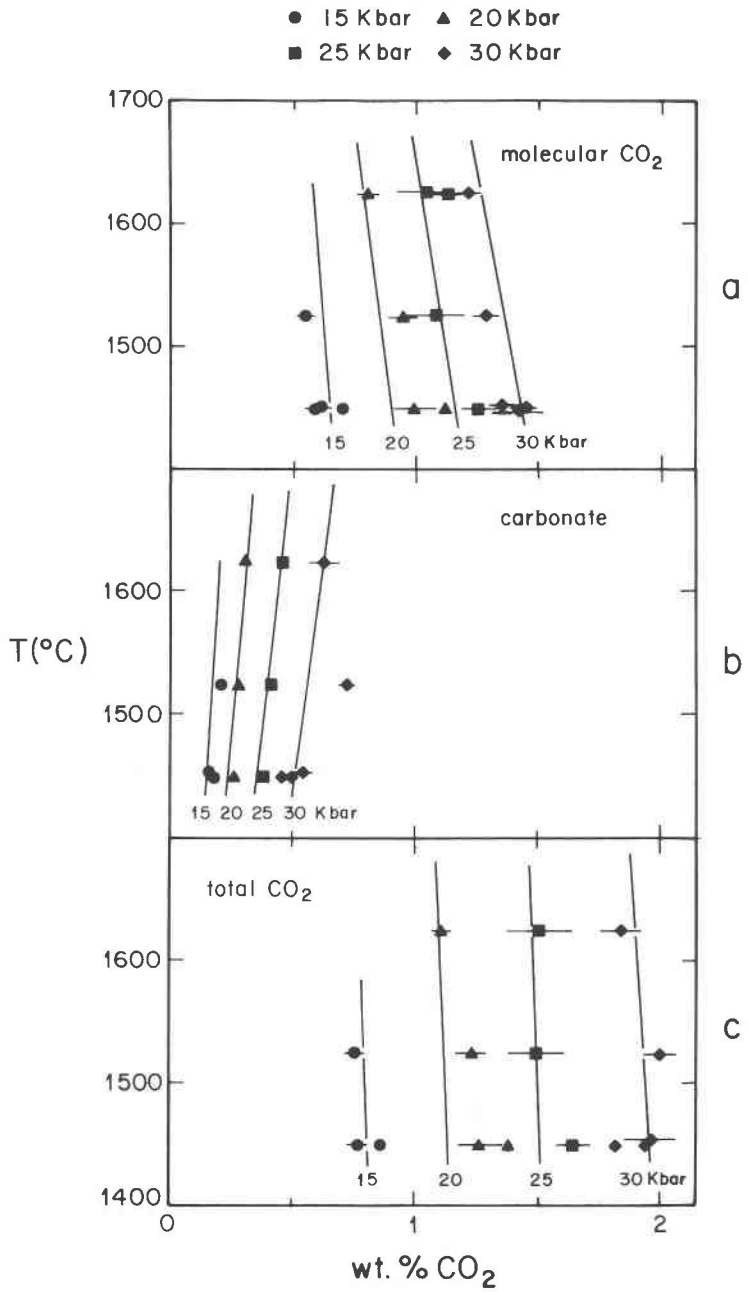

Fig. 4. (a) Molecular CO_2, (b) CO_2 dissolved as carbonate, and (c) total CO_2 concentrations vs. temperature for CO_2-saturated albitic melts. Error bars are 1σ for the distribution of measurements for each sample; when only one measurement was available or the error is smaller than the symbol, no error bar is shown. See Table 3 for the errors on each measurement. Lines are calculated values based on the fits to Equations 4 and 7.

The effects of water. Two pairs of experiments equilibrated at the same temperatures and pressures (TJ-37 and TJ-48; TJ-41 and ALB2965) contain different amounts of dissolved water, yet their dissolved molecular CO_2 and carbonate contents and hence their total dissolved CO_2 contents are, within error, the same. This suggests that at least at low water contents, CO_2 solubility and speciation are not strongly dependent on water content.

We note that the water contents of all of our run products are disturbingly high. We have discussed the possible sources of this water in these nominally anhydrous runs at length previously (Fine and Stolper, 1985, and above). We reiterate that we believe that it is unavoidable in piston-cylinder experiments because of a combination of adsorbed water on the starting materials (particularly the silver oxalate) and diffusion of hydrogen into the capsules during run conditions. We doubt that previous studies of

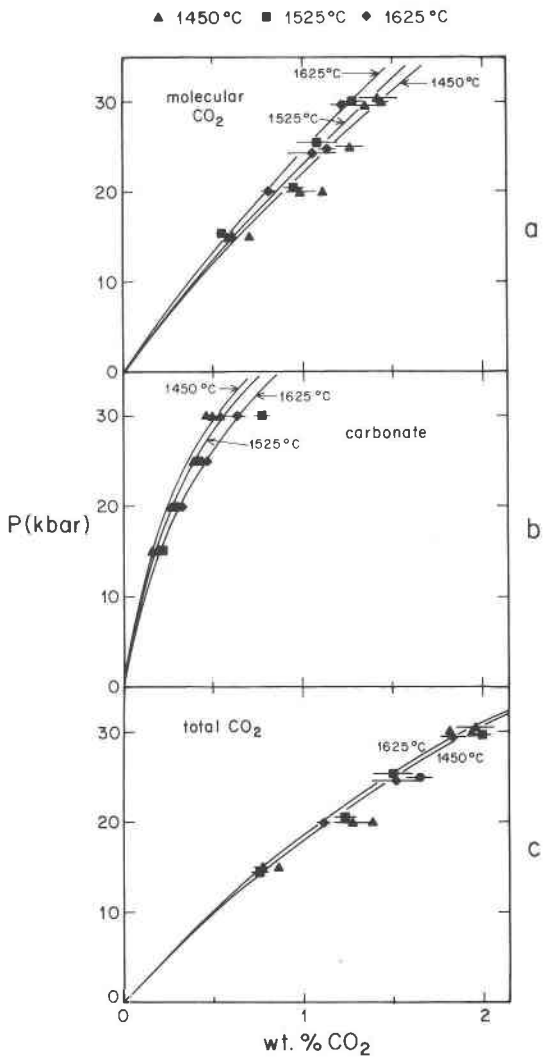

Fig. 5. (a) Molecular CO_2, (b) CO_2 dissolved as carbonate, and (c) total CO_2 concentration vs. pressure for CO_2-saturated albitic melts. Error bars as discussed for Fig. 4. Curves are calculated values based on the fits to Equations 4 and 7.

CO_2 solubility using analogous methods of glass preparation have been successful in establishing anhydrous conditions either.

Sample heterogeneity. For most samples, spectra were obtained on several different bubble-free regions of the glass, allowing us to assess sample homogeneity. Table 3 lists the number of spots analyzed for each species on each sample. The standard deviation of the distribution of analyses is typically similar to their precision, indicating that the samples are usually homogeneous to the level that we are capable of determining. There are a few exceptions, but only in a few cases is the standard deviation greater than about 10% of the value of the mean. Note that the homogeneity of the vapor-saturated samples contrasts with the marked zoning of undersaturated experiments (see Fig. 3). CO_2 may have been lost continuously by reduction in the vapor-saturated experiments much as it was in the undersaturated experiments, but the excess CO_2 present in bubbles throughout the vapor-saturated experiments probably approximately buffered the activity of CO_2 in these experiments.

Achievement of equilibrium. The experiments were not reversed, so equilibrium has not been proved. However, our run lengths were 1–1.5 h, greatly in excess of the 10 min or so that Mysen (1976) demonstrated to be sufficient to reach a time-independent result, which he inferred to be indicative of the attainment of equilibrium. The two vapor-saturated experiments included in this study that were conducted by A. L. Boettcher (ALB2965 and 2998) were held at pressure and temperature for 2 and 3 h, respectively, and are similar to our 1-h experiment (TJ-41) held at the same run conditions.

Molecular CO_2: dissolved or in bubbles? We are frequently asked if we can be certain that the molecules of CO_2 that we detect spectroscopically are dissolved in the glass rather than present as bubbles or inclusions. Spectra were obtained only on regions of glass that, on the basis of examination with an optical microscope, are bubble-free or contain no more than a handful of bubbles. With the help of Ian Hutcheon, we have demonstrated with a scanning-electron microscope that regions that appear bubble-free with an optical microscope are free of bubbles down to a scale of a few hundred ångströms. In addition, we have demonstrated, as described above, that the infrared spectra of CO_2 bubble–rich samples differ significantly from those of optically bubble-free samples at room temperature, and that the spectra of bubble-free samples show negligible changes between room temperature and liquid-nitrogen temperature whereas bubble-rich specimens show dramatic changes over this temperature range, presumably owing to the freezing of the CO_2 in the bubbles. Unfortunately, these observations only rule out the presence of CO_2 in relatively large (100 Å?) bubbles. We cannot prove that molecular CO_2 is not present in smaller clusters that are not readily visible and do not behave like a bulk, separate phase. However, since dissolved CO_2 molecules would probably be located in "holes" in the melt structure and possibly in clusters, at this level the distinction between bubbles and dissolved CO_2 may be a semantic one. Nevertheless, the simple patterns in our results [e.g., regularities in the concentration of molecular CO_2 with pressure and temperature and in the ratio of molecular CO_2 to carbonate with pressure, temperature, and melt chemistry (Fine and Stolper, 1985)] strongly suggest that the concentrations of molecular CO_2 that we observe are controlled by thermodynamics, rather than by the vagaries of some mechanism of physical entrapment.

Thermodynamic treatment

Our data can be used to constrain a thermodynamic description of the solubility of CO_2 in silicate melts, in much the same way that Spera and Bergman (1980) did for previous measurements of CO_2 solubility in silicate melts. However, in that case, only bulk solubility was

considered, whereas our data permit a separation of the heterogeneous equilibrium between melt and vapor and the homogeneous equilibrium between C-bearing species in the melt.

Vapor-melt equilibrium

Let us first consider the heterogeneous equilibrium between CO_2 in the vapor and molecular (mol.) CO_2 in the melt. This may be described by the reaction

$$CO_2(\text{vapor}) = CO_2,\text{mol.}(\text{melt}). \quad (1)$$

The condition of equilibrium is

$$\mu_{CO_2}^{\text{vapor}} = \mu_{CO_2,\text{mol.}}^{\text{melt}}. \quad (2)$$

This can be readily modified into the following relation that allows the activity of molecular CO_2 in melt saturated with CO_2 vapor at any P and T to be calculated provided that it is known at some reference pressure (P_0) and temperature (T_0):

$$a_{CO_2,\text{mol.}}^{\text{melt}}(P, T) = a_{CO_2,\text{mol.}}^{\text{melt}}(P_0, T_0)\frac{f_{CO_2}(P, T)}{f_{CO_2}(P_0, T_0)} \cdot \exp\left\{-\frac{V_{CO_2,\text{mol.}}^{0,\text{melt}}(P - P_0)}{RT} - \frac{\Delta H^0(P_0)}{R}\left[\frac{1}{T} - \frac{1}{T_0}\right]\right\}, \quad (3)$$

where $a_{CO_2,\text{mol.}}^{\text{melt}}(P, T)$ and $a_{CO_2,\text{mol.}}^{\text{melt}}(P_0, T_0)$ are the activities of molecular CO_2 in the vapor-saturated melt at P and T and at P_0 and T_0, respectively, relative to a standard state of pure CO_2 molecules at the pressure and temperature of interest (Fine and Stolper, 1985); $f_{CO_2}(P, T)$ and $f_{CO_2}(P_0, T_0)$ are the fugacities of CO_2 in the vapor at P and T and at P_0 and T_0; $V_{CO_2,\text{mol.}}^{0,\text{melt}}$ is the molar volume of molecular CO_2 in the melt in its standard state and has been taken to be independent of P and T in deriving Equation 3; $\Delta H^0(P_0)$ is $H^0(CO_2,\text{mol.},\text{melt}) - H^0(CO_2,\text{vapor})$ at P_0 and T_0, where $H^0(CO_2,\text{vapor})$ is the enthalpy per mole of CO_2 vapor at a pressure sufficiently low for the vapor phase to be perfect at T_0 and $H^0(CO_2,\text{mol.},\text{melt})$ is the molar enthalpy of molecular CO_2 in the melt in its standard state at P_0 and T_0. Note that in deriving Equation 3, ΔH^0 has been assumed to be independent of temperature, but it is a function of pressure [$\Delta H^0(P) = \Delta H^0(P_0) + V_{CO_2,\text{mol.}}^{0,\text{melt}}(P - P_0)$].

Assuming that the melt can be treated as an ideal mixture of CO_2 molecules, carbonate groups, and oxygen atoms (Fine and Stolper, 1985), we have

$$a_{CO_2,\text{mol.}}^{\text{melt}}(P, T) = X_{CO_2,\text{mol.}}^{\text{melt}}(P, T)$$
$$a_{CO_3^{2-}}^{\text{melt}}(P, T) = X_{CO_3^{2-}}^{\text{melt}}(P, T)$$
$$a_{O^{2-}}^{\text{melt}}(P, T) = X_{O^{2-}}^{\text{melt}}(P, T),$$

where the mole fraction of each species is simply the number of moles of that species in the melt divided by the total number of moles of all three species in the melt (see Fine and Stolper, 1985). This choice of activity-composition relationship is analogous to the one we have used for water-bearing melts (Stolper, 1982b; Silver and Stolper, 1985). It is unambiguous since it is independent of the formula unit chosen for the C-free silicate, but it does not take into account the difference in size between the various species, the facts that there are probably many distinguishable sorts of oxygens in the melt and that they probably mix as polymeric groups rather than as individuals, and that CO_2 may mix on sites different from the other species. However, the particular choice of activity-composition relationship will probably make little difference in the determination of the thermodynamic parameters since the concentrations of C-bearing species are low.

Given this choice of activity-composition relationship, Equation 3 becomes

$$X_{CO_2,\text{mol.}}^{\text{melt}}(P, T) = X_{CO_2,\text{mol.}}^{\text{melt}}(P_0, T_0)\frac{f_{CO_2}(P, T)}{f_{CO_2}(P_0, T_0)} \cdot \exp\left\{-\frac{V_{CO_2,\text{mol.}}^{0,\text{melt}}(P - P_0)}{RT} - \frac{\Delta H^0(P_0)}{R}\left[\frac{1}{T} - \frac{1}{T_0}\right]\right\}, \quad (4)$$

where $V_{CO_2,\text{mol.}}^{0,\text{melt}}$ is now the partial molar volume of molecular CO_2 in the melt and $H^0(CO_2,\text{mol.},\text{melt})$ is now the partial molar enthalpy of molecular CO_2 in the melt. If we know $X_{CO_2,\text{mol.}}$ for a vapor-saturated melt at a reference pressure and temperature and have values for $V_{CO_2,\text{mol.}}^{0,\text{melt}}$ and for ΔH^0 at the reference pressure, Equation 4 can be used to calculate $X_{CO_2,\text{mol.}}^{\text{melt}}$ in vapor-saturated albitic melt at any other P and T.

Using our data on the concentrations of molecular CO_2 and carbonate as a function of P and T and the modified Redlich-Kwong equation of state of CO_2 vapor (Holloway, 1977), we have obtained values for the parameters in Equation 4 by least squares. These values are given in Table 4. The reference temperature and pressure were taken as 1450 °C and 20 kbar. The partial molar volume of molecular CO_2 given by this regression is 28.6 cm³/mol. This is somewhat lower than the value of 33–35 cm³/mol determined by Spera and Bergman (1980) for the partial molar volume of CO_2 in albitic melt based on the data Mysen et al. (1976). It is also lower than the molar volume of the CO_2 vapor under these conditions (34–40 cm³/mol), but similar to the b parameter for CO_2 molecules in the Redlich-Kwong equation of state (29.7 cm³/mol).

Molecular CO_2-carbonate equilibrium

Let us now consider the homogeneous equilibrium between CO_2 molecules, carbonate groups, and the silicate framework in albitic melt. We will describe this via the following reaction:

$$CO_2,\text{mol.}(\text{melt}) + O^{2-}(\text{melt}) = CO_3^{2-}(\text{melt}). \quad (5)$$

TABLE 4. Best-fit thermodynamic parameters for Equations 4 and 7

CO_2(vapor) = CO_2,molecular(melt)
P_0 = 20 kbar
T_0 = 1450 °C
$X^{melt}_{CO_2,mol}$ (P_0, T_0) = 0.0067 ± 0.0002
$V^{0,melt}_{CO_2,mol}$ (P, T) = 28.6 ± 0.5 cm³/mol
ΔH^0 (P_0) = 9200 ± 1600 cal/mol
CO_2,molecular(melt) + O^{2-}(melt) = CO_3^{2-}(melt)
P_0 = 20 kbar
T_0 = 1450 °C
K_C (P_0, T_0) = 0.27 ± 0.01
ΔV^0_r (P, T) = −3.9 ± 0.8 cm³/mol
ΔH^0_r (P_0) = 13500 ± 3000 cal/mol

We recognize this as a gross oversimplification since it does not specify the structural changes that take place in the silicate framework of the melt as this reaction proceeds. In the absence of any concrete information on the details of this reaction, we will describe the homogeneous equilibria with this generalized equation plus the assumption of ideal mixing of the CO_2 molecules, carbonate groups, and oxygen atoms described above. Though this treatment, in which basically all of the oxygens in the melt will be considered to be indistinguishable and equally available for reaction with molecules of CO_2, is an oversimplification, the thermodynamic parameters derived from it are not expected to depend strongly on the details because the concentrations of the C-bearing species are low (Fine and Stolper, 1985); that is, similar derivative parameters (e.g., ΔV, ΔH) would be obtained regardless of the details of the reactions being modeled.

The condition for equilibrium for Reaction 5 is

$$\mu^{melt}_{CO_2,mol.} + \mu^{melt}_{O^{2-}} = \mu^{melt}_{CO_3^{2-}} \quad (6)$$

This can be rearranged to give

$$K_C(P, T) = K_C(P_0, T_0)\exp\left\{-\frac{\Delta V^0_r(P - P_0)}{RT} - \frac{\Delta H^0_r(P_0)}{R}\left[\frac{1}{T} - \frac{1}{T_0}\right]\right\}, \quad (7)$$

where

$$K_C = \frac{a^{melt}_{CO_3^{2-}}}{a^{melt}_{CO_2,mol.}\, a^{melt}_{O^{2-}}} = \frac{X^{melt}_{CO_3^{2-}}}{X^{melt}_{CO_2,mol.}\, X^{melt}_{O^{2-}}}, \quad (8)$$

P_0(bars) and T_0(K) are a reference pressure and temperature; P and T are some other pressure and temperature; ΔV^0_r is the volume change of the components of Reaction 5 in their standard states, which is equal to the volume change of the reaction given our assumption of ideal mixing and was taken to be independent of P and T in deriving Equation 7; $\Delta H^0_r(P_0)$ is the change in enthalpy of the components of Reaction 5 in their standard states at P_0, which is equal to the enthalpy change of the reaction at P_0 given the assumption of ideal mixing. ΔH^0_r was assumed to be independent of temperature in deriving Equation 7, but it is a function of pressure.

Using our data on the concentrations of molecular CO_2 and carbonate as a function of P and T, we have obtained values for the parameters in Equation 7 by least squares. These values are given in Table 4. The reference temperature and pressure were taken as 1450 °C and 20 kbar. The negative volume change of this reaction and the positive enthalpy change are reflections of the increases in the carbonate to molecular CO_2 ratio observed with increasing pressure and temperature.

Calculation of CO_2 solubility and speciation in albitic melts

The parameters given in Table 4 can be used to calculate CO_2 solubility and speciation in vapor-saturated albitic melts as a function of pressure and temperature. First, Equation 4 is used to calculate $X_{CO_2,mol.}$ for a given set of values of P, T, and f_{CO_2}. Then, Equation 7 is used to calculate K_C at this P and T. Given $X^{melt}_{CO_2,mol.} + X^{melt}_{CO_3^{2-}} + X^{melt}_{O^{2-}} = 1$, and the value of $X^{melt}_{CO_2,mol.}$ derived from Equation 4, the calculated value of K_C can be readily used to determine $X^{melt}_{O_3^{2-}}$ and $X^{melt}_{O^{2-}}$.

Weight percentages of molecular CO_2 and of CO_2 dissolved as carbonate as well as total dissolved CO_2 contents were calculated for the pressure and temperature range covered by our experiments using the parameters given in Table 4 and compared to our measured values in Figures 4 and 5. Not surprisingly, since these were the data used to constrain the thermodynamic parameters given in Table 4, the calculations are a good fit to the data; the mean of the absolute value of the deviation between measured and calculated molecular CO_2 concentrations is about 0.07 wt% and for carbonate it is about 0.03 wt%. These deviations are comparable to our precision at a 1σ level. The maximum deviations (0.22 wt% for molecular CO_2 and 0.06 wt% carbonate [except for TJ-40, which was excluded from the fitting procedure]) are at the 2σ to 3σ level.

The calculated total CO_2 solubility at 1 bar and 1450 °C is about 0.5 ppm by weight, about 90% of which is dissolved as molecules of CO_2.

Calculation of the CO_2-saturated solidus of albite

Using the procedures and data given in Silver and Stolper (1985) plus the parameters listed in Table 4, we have calculated the effect of CO_2 on the melting of crystalline albite. The calculated freezing-point depression (i.e., the difference in temperature between the dry solidus and the beginning of melting of albite in the presence of CO_2 vapor) increases from 4 °C at 5 kbar, to 13 °C at 15 kbar, to 25 °C at 25 kbar. These values are consistent with the data reported by Eggler and Kadik (1979) and Boettcher et al. (1987).

COMPARISON WITH PREVIOUS STUDIES

There have been several previous studies of CO_2 solubility in albitic melts. Mysen et al. (1976) used both

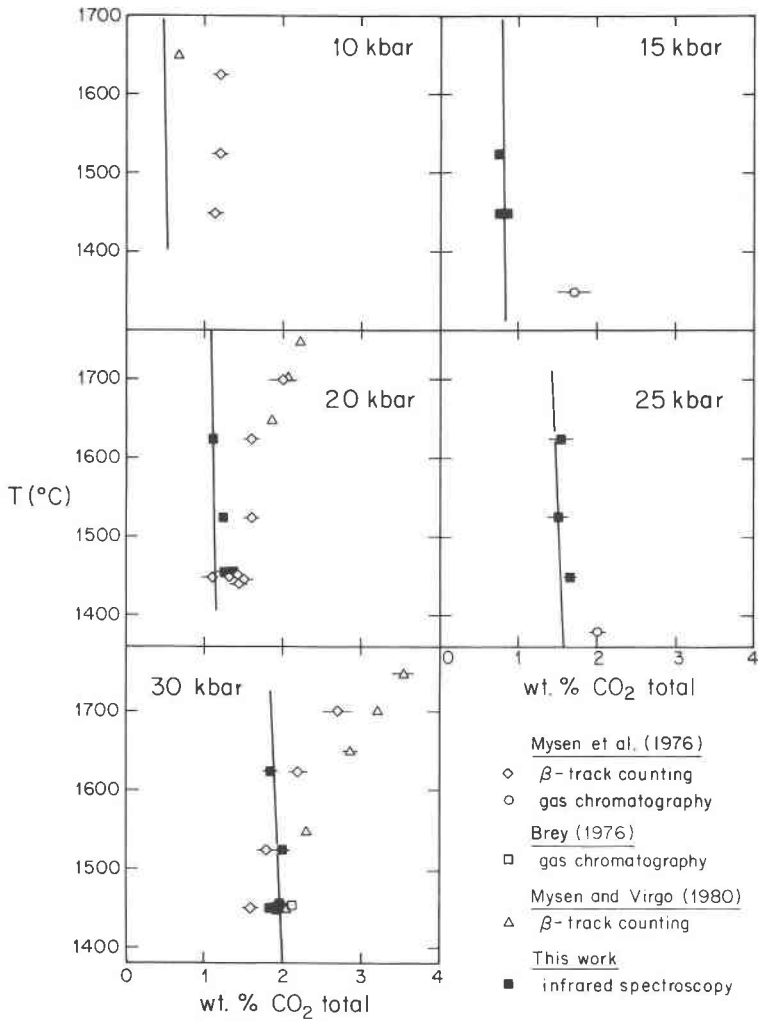

Fig. 6. Total CO_2 solubility vs. temperature for various pressures from this work and the literature. Error bars from this work as described for Fig. 4. Error bars from Mysen et al. (1976) and Mysen and Virgo (1980) are as reported by them in their data tables. Lines are calculated values based on the fits to Equations 4 and 7.

β-track radiography and gas chromatography to measure CO_2 solubility in albitic melts at 5–30 kbar and 1350–1700 °C. In a companion paper, Mysen (1976) reported molecular CO_2 and carbonate concentrations based on infrared spectroscopy. Brey (1976) reported a single measurement at 1450 °C and 30 kbar using gas chromatography and also reported some infrared spectroscopic results. Mysen and Virgo (1980) used β-track radiography to measure CO_2 solubility at 10–30 kbar and 1450–1750 °C; they used Raman spectroscopy to measure relative molecular CO_2 and carbonate concentrations.

All previous measurements of total CO_2 solubility under nominally anhydrous conditions, which should be directly comparable to our results, are shown in Figure 6 along with our data and our best-fit solubility function based on the parameters given in Table 4. Measurements of molecular CO_2 and carbonate concentrations from this study are compared with those of Mysen (1976) in Figure 7. In this section, we discuss these different data sets.

Total solubility measurements. As shown in Figure 6, there is a conspicuous lack of correspondence between the several reports of total CO_2 solubility in albitic melts. In general, our values are less than those of Mysen et al. (1976) and Mysen and Virgo (1980), but the deviations are not systematic. For example, at 1450 °C and 30 kbar, there is reasonable agreement between the four reported values: 1.6 wt% (Mysen et al., 1976), 2.1 wt% (Brey, 1976), 2.06 wt% (Mysen and Virgo, 1980), and 1.8–2.0 wt% based on three experiments from this study. Similarly, at 1525–1550 °C and 30 kbar, our value of 2.0 wt% is bracketed by the values of 1.8 wt% reported by Mysen et al. (1976) and 2.31 wt% reported by Mysen and Virgo (1980). However, under most other conditions, our values tend to be lower than those of Mysen et al. (1976) and Mysen and Virgo (1980), even excluding the gas chromatographic values that Mysen et al. (1976) rejected as probably being too high because of trapped bubbles.

We have considered several possible explanations for

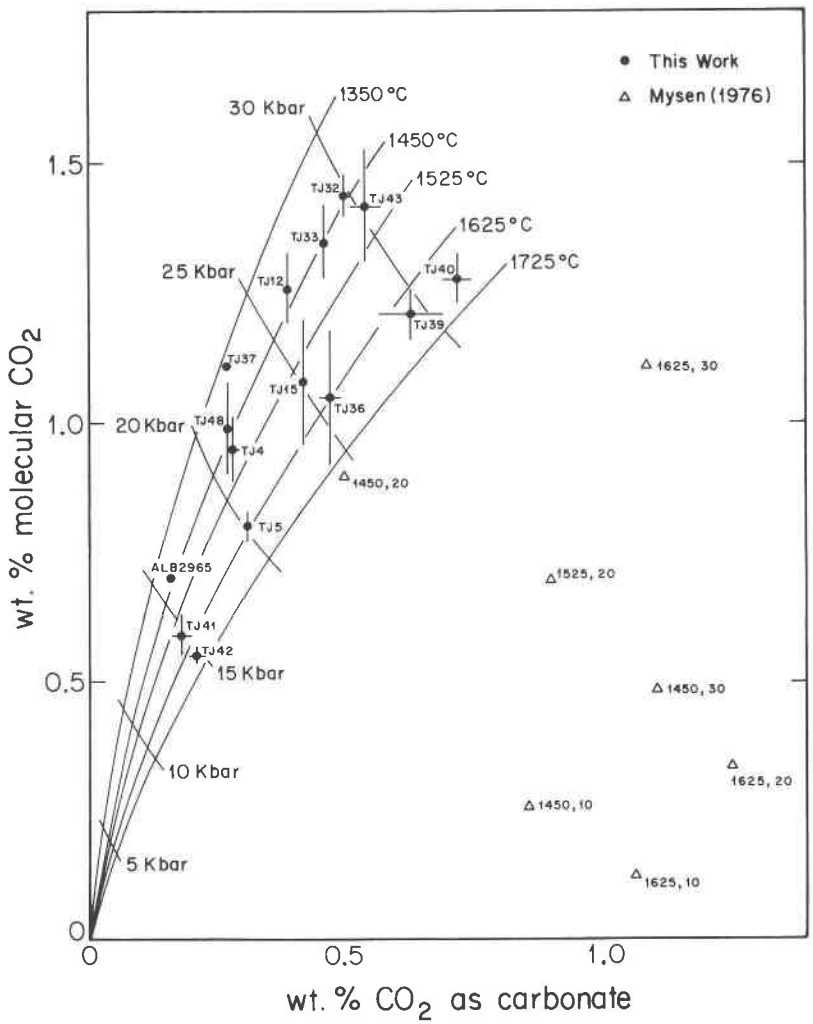

Fig. 7. Molecular CO_2 vs. carbonate concentrations for CO_2-saturated albitic melts from this work and Mysen (1976). Curves are calculated isotherms and isobars based on the fits to Equations 4 and 7. Error bars as described for Fig. 4. Note the wide scatter in the results of Mysen (1976) compared to those in this work.

the differences between our results and those of Mysen et al. (1976) and Mysen and Virgo (1980) that would reflect problems with our experiments or analyses: (1) The fact that we obtain similar results whether we analyze our experiments or those conducted by A. L. Boettcher suggests that differences are not due to some peculiarity of our solid-media apparatus or of our starting material. We note that run number ALB2998 (15 kbar, 1450 °C, 1% CO_2 loaded) contains widespread bubbles up to 30 μm in diameter, suggesting—in agreement with our results but conflicting with those of Mysen and his co-workers—a solubility of less than 1 wt% CO_2 under these conditions. The presence of uncommon, small ($\lesssim$10–μm diameter) bubbles in AL2995 (20 kbar, 1450 °C, 1% CO_2 loaded) would suggest solubilities even lower than those we have reported for 20 kbar, but rare, small bubbles may not necessarily reflect vapor saturation (Burnham and Jahns, 1962). (2) Our experiments were run much longer than those of Mysen and his co-workers, but it is hard to see how this would lead to lower values under some conditions but not under others. (3) If there were problems with our calibration, deviations would be expected to be systematic. (4) A final possibility is that under some conditions there are forms of C other than molecular CO_2 and carbonate dissolved in our glasses that we fail to detect by infrared spectroscopy. We note that if the mystery species were a reduced form of C, this could explain the zoning and in particular the apparent C-deficiency observed near the rims of undersaturated experiments (Fig. 2). However, if a mystery species is the reason for the observed deviations, its concentration does not appear in vapor-saturated samples to be correlated with dissolved water content (as would be expected if it were related to an influx of H) and would have to be highest at low pressures and at high temperatures.

There is nothing obviously wrong with either our measurements or those of Mysen et al. (1976) and Mysen and Virgo (1980) using β-track radiography, so the cause of

the deviations between these two data sets cannot be assigned. We note, however, that contrary to the statement in Mysen and Virgo (1980), their data are not in very good agreement with the earlier measurements by the same technique first reported by Mysen et al. (1976). This is apparent in Figure 6, where experiments conducted under identical conditions have CO_2 concentrations measured by Mysen and his co-workers differing by more than 0.5 wt% and experiments conducted under similar conditions (i.e., differing in temperature by 50 °C) differ by almost 0.9 wt%. At 10 kbar, the earlier solubilities are the high ones; at 30 kbar it is the reverse. There clearly is some lack of reproducibility in the CO_2 solubilities reported by this group. Since our solubility values typically deviate from theirs by 0.5 wt% or less, perhaps the deviations between our data sets reflect the fact that the precision of the β-track measurements is poorer than has been reported.

In summary, we are reasonably confident of our results, and there appears to be a lack of reproducibility in the β-track results reported by Mysen et al. (1976) and Mysen and Virgo (1980). Nevertheless, we cannot track down with certainty the cause of the discrepancies between our results and those in the literature and conclude that this will only be resolved through the use of an independent technique for measuring dissolved CO_2 contents.

Temperature dependence of solubility. As shown in Figures 4 and 6, our results show a negligible to slightly negative dependence of total CO_2 solubility on temperature. A similar result was inferred by Brey (1976) for albitic melt. Similar results have been found in investigations of CO_2 solubility in several other silicate melt compositions (Pearce, 1964; Faile and Roy, 1966; Sharma, 1979; Rai et al., 1983). Mysen et al. (1976) found a similar result at about 10 kbar for albitic melt, but found a strong positive temperature dependence of CO_2 solubility at higher pressures (Fig. 6). We have found no simple explanation for the discrepancy between our results and those of Mysen et al. (1976) and Mysen and Virgo (1980) and again suggest that an independent technique be used to resolve it, while pointing out that the results of these two studies by Mysen and his co-workers using identical techniques are not entirely consistent given their reported error bars.

Molecular CO_2 vs. carbonate concentrations. We have found that pressure and temperature have an effect on the ratio of dissolved molecular CO_2 to carbonate (i.e., ΔH_r^0 and ΔV_r^0 are nonzero in Eq. 7). However, as shown in Figure 7, the variations in this ratio with pressure and temperature are gradual and small compared to the results of Mysen (1976). We had previously concluded (Fine and Stolper, 1985), on the basis of data from glasses with lower total CO_2 concentrations than those studied by Mysen (1976), that the large range in CO^2/CO_3^{2-} ratios that he reported and the nongradual changes that he found in this ratio with pressure and temperature were artifacts of his use of the imprecise KBr pellet technique for his infrared determinations of carbonate concentrations, and we reiterate that conclusion here. Our results do not support the earlier suggestions (Mysen, 1976; Mysen et al., 1976) that there are abrupt changes in melt polymerization over the 15–30-kbar range that lead to dramatic changes in CO_2 speciation and solubility. Our results indicate that there is a subtle, gradual increase in the ratio of carbonate to molecular CO_2 over this pressure range and that most of the increase in total CO_2 solubility is due to the increasing concentration of molecular CO_2 driven by the difference in volume between CO_2 in the vapor and CO_2 molecules in the melt.

The effects of water on CO_2 solubility. Previous studies have indicated that CO_2 solubility in albitic melt increases by about 0.8 wt% when the water content increases from zero to about 8–9 wt% (Eggler, 1973; Mysen, 1976; Eggler and Kadik, 1979). This is thought to be due to increased concentrations of dissolved carbonate complexes under hydrous conditions. Our data show no detectable enhancement of molecular CO_2 solubility or carbonate concentration under vapor-saturated conditions as the dissolved water content increases from about 0.1 to 0.7 wt%. If the increase is CO_2 solubility were linear with water content, the CO_2 content would be expected to increase by about 0.05 wt% as the water content increases from 0.1 to 0.7 wt%; this could probably be detected if the increase were entirely in the carbonate concentration. More work will be needed to determine the exact nature of the relationship between dissolved water and CO_2 contents of vapor-saturated melts at low water contents.

Discussion

Given the unexplained discrepancies between our measurements of CO_2 solubility and those of Mysen et al. (1976) and Mysen and Virgo (1980), we are reluctant to overinterpret the details of our results. There are, however, two important points that we believe will stand independent of the resolution of these discrepancies.

The first is that understanding of the total solubility of a volatile component such as CO_2 depends critically on an understanding of the speciation of this component in the melt. Because the total solubility of CO_2 is the sum of the CO_2 dissolved as molecules of CO_2, as carbonate, and perhaps in other forms as well, modeling of the variations in solubility of CO_2 must consider the effects of temperature, pressure, and melt composition both on the equilibria between vapor and molecular CO_2 and between the various dissolved species. For example, in albitic melt the solubility of molecular CO_2 decreases with increasing temperature, the concentration of carbonate in equilibrium with the dissolved molecular CO_2 increases with increasing temperature, and the sum—the total solubility of CO_2—displays almost no temperature dependence. However, in other melt compositions, the competition between the temperature dependencies of Reactions 1 and 5 may balance out differently. For example, in molten SiO_2, which probably dissolves CO_2 nearly entirely as molecular CO_2 (Fine and Stolper, 1985), there will be no

carbonate with its concentration showing a positive temperature dependence, so a negative temperature dependence of solubility would be expected. In contrast, for jadeitic and nephelinitic melts, in which carbonate dominates over molecular CO_2, the positive temperature dependence of dissolved carbonate concentration could overwhelm the negative temperature dependence of the concentration of the minor species, molecular CO_2, with the net result being a positive temperature dependence of the bulk CO_2 solubility.

Treatments of the solubilities of other volatile components such as water and SO_2 that can dissolve both as molecular species and as species formed by reaction with the silicate framework (e.g., hydroxyl groups, sulfate groups) will require similar considerations both of heterogeneous equilibia between vapor and molecular species in the melt and of homogeneous equilibria between melt species. In most cases, the temperature dependence of the solubility of the molecular species is expected to be negative, reflecting the usually positive enthalpy of vaporization of such species (i.e., things usually boil when heat is added to them). For very large molecular species, however, the temperature dependence may well be positive, reflecting the energetic costs of forcing such molecules (or atoms, in the case of the heavy rare gases) into holes in the melt structure into which they do not quite fit. In addition, the difference in enthalpy between these molecular species in the gas phase and in the melt, even if positive at low pressure, will tend to decrease as pressure increases from 1 bar, so that the temperature dependence tends to become less negative, and may even become positive, as pressure increases. Indeed, the temperature dependence of water solubility may switch from negative to positive with increasing pressure (e.g., Kennedy et al., 1962; Khitarov and Kadik, 1973), and this could reflect such an effect. In any case, the temperature dependence of water solubility reflects a competition between the solubility of molecular H_2O and the homogeneous equilibria between molecular water and hydroxyl groups, which are probably favored by increasing temperature (Stolper et al., 1983), and thus is probably similar to the case we have described for CO_2 solubility.

The second point that we want to make has to do with the pressure dependence of CO_2 solubility. Note in Figure 5 that the solubility of CO_2 does not increase linearly with pressure, as is often supposed to be its normal behavior (e.g., Harris, 1981; Des Marais and Moore, 1984). In fact, according to our results, the rate of increase in solubility increases with increasing pressure over the pressure range that we have investigated. Although a small part of this shape is due to the increasing ratio of carbonate to molecular CO_2 with increasing pressure (i.e., to the negative ΔV_r^0 of Reaction 5), this shape is also observed for the molecular CO_2 solubility.

We would be mistaken if we interpreted this as unusual behavior reflecting changes in melt structure over this pressure range (e.g., Mysen, 1976). In fact, note that the calculated molecular CO_2 solubility based on Equation 4 and the parameters given in Table 4 also display this behavior. The second derivative of the activity of a molecular species (in vapor-saturated melt) with respect to pressure is given by

$$\frac{d^2a}{dP^2} = a\left[\frac{1}{RT}\frac{dV^v}{dP} + \left(\frac{V^v - V^m}{RT}\right)^2\right], \tag{9}$$

where V^v is the molar volume of the vapor and V^m is the molar volume of the molecular species in the melt in its standard state (which is taken as a fictive form of the pure molecular species at P and T). If the partial molar volume of the species in the melt is zero and the gas is ideal, the second derivative is zero, and the activity of the species is proportional to pressure. If the partial molar volume is positive and the gas is ideal, the second derivative will be negative at pressures less than $2RT/V^m$. At elevated pressures where the gas is nonideal, though the first term in Equation 9 is always negative, it becomes small and if the partial molar volume of the species in the melt is small relative to the molar volume of the vapor, the second term, which is always positive, overwhelms the first and the second derivative is positive. Based on our data, the partial molar volume of molecular CO_2 (28.6 cm^3/mol) is small relative to the volume of the vapor in the 15–30-kbar range; consequently, the second derivative is positive in this pressure range. The point is that the shapes of solubility curves and other phase boundaries can only with difficulty be used to infer microscopic behaviors and that, in particular, the rapid increase in CO_2 solubility observed between 15 and 30 kbar does not necessarily signal anomalous changes in melt structure or polymerization over this pressure range.

Summary

1. Infrared spectroscopy has been used to measure dissolved molecular CO_2, carbonate, and water concentrations of albitic glasses quenched from melts equilibrated with CO_2-rich vapor at 15–30 kbar and 1450–1625 °C.

2. At constant temperature, the molecular CO_2 and the carbonate concentrations of vapor-saturated albitic melts increase with increasing pressure. For each species and their sum (i.e., the total dissolved CO_2), the second derivative of concentration with respect to pressure is positive over the 15–30-kbar range. The ratio of molecular CO_2 to carbonate dissolved in albitic melts decreases with increasing pressure at constant temperature.

3. At constant pressure, the concentration of molecular CO_2 in vapor-saturated albitic melts decreases with increasing temperature, but the concentration of carbonate increases. The sum of the concentration of these two species (i.e., the total dissolved CO_2 concentration) is approximately independent of temperature at constant pressure under the conditions that we have investigated.

4. Thermodynamic analysis of the solubility data that we have presented requires the consideration of two equilibria. The first, CO_2(vapor) = CO_2,mol.(melt) (Reaction 1), describes heterogeneous equilibrium between vapor and melt. The second, CO_2,mol.(melt) + O^{2-}(melt) = CO_3^{2-}(melt) (Reaction 5), describes homogeneous equilib-

rium between melt species. Our data on the variations in the concentrations of dissolved molecular CO_2 and carbonate under vapor-saturated conditions can be well described by Reactions 1 and 5 if at 20 kbar and 1450 °C, the partial molar volume of molecular CO_2 in albitic melt is 28.6 cm^3/mol, the difference in enthalpy between dissolved molecular CO_2 and pure CO_2 gas at low pressure is 9.2 kcal/mol, the volume change of Reaction 5 is −3.9 cm^3/mol, and the enthalpy change of Reaction 5 is 13.5 kcal/mol.

5. There are significant, nonsystematic discrepancies between CO_2 solubility in albitic melt and its pressure and temperature dependence as measured by us and as measured using β-track radiography by Mysen et al. (1976) and Mysen and Virgo (1980). These will have to be resolved by future work. The reports by Mysen (1976) of substantial variations in the ratio of molecular CO_2 to carbonate in CO_2-saturated albitic glasses in the pressure and temperature range investigated in this study can, however, be discounted. This ratio varies gradually over this range of conditions and only by relatively small amounts. Our data do not suggest major or abrupt changes in melt structure or polymerization over this range of conditions.

Acknowledgments

We thank George Rossman for his cooperation and Paula Rosener for her help with the FTIR. The interest and assistance of A. Boettcher, J. T. Cheney, and J. R. Holloway are appreciated. Ian Hutcheon generously helped us with SEM examination of our glasses. This work was began under an Undergraduate Summer Internship (to T.J.) in the Division of Geological and Planetary Sciences, Caltech, and was the basis of an honors thesis submitted to Amherst College. The research was supported by NSF Grants EAR-8212765 and EAR-8417434, Caltech Division of Geological and Planetary Sciences Contribution Number 4274.

References cited

Boettcher, A.L., Luth, R.W., and White, B.S. (1987) Carbon in silicate liquids: The systems $NaAlSi_3O_8$-CO_2, $CaAl_2Si_2O_8$-CO_2, and $KAlSi_3O_8$-CO_2. Contributions to Mineralogy and Petrology, in press.

Brey, G. (1976) CO_2 solubility and solubility mechanisms in silicate melts at high pressures. Contributions to Mineralogy and Petrology, 57, 215–221.

Burnham, C.W., and Jahns, R.H. (1962) A method for determining the solubility of water in silicate melts. American Journal of Science, 260, 721–745.

Des Marais, D.J., and Moore, J.G. (1984) Carbon and its isotopes in mid-oceanic basaltic glasses. Earth and Planetary Science Letters, 69, 43–57.

Eggler, D.H. (1973) Role of CO_2 in melting processes in the mantle. Carnegie Institution of Washington Year Book 72, 457–467.

Eggler, D.H., and Kadik, A.A. (1979) The system $NaAlSi_3O_8$-H_2O-CO_2 to 20 kbar pressure: I. Compositional and thermodynamic relations of liquids and vapors coexisting with albite. American Mineralogist, 64, 1036–1048.

Faile, S.P., and Roy, D.M. (1966) Solubilities of Ar, N_2, CO_2 and He in glasses at pressures to 10 kbars. American Ceramic Society Journal, 49, 638–643.

Fine, G., and Stolper, E. (1985) The speciation of carbon dioxide in sodium aluminosilicate glasses. Contributions to Mineralogy and Petrology, 91, 105–121.

——— (1986) Dissolved carbon dioxide in basaltic glasses: Concentrations and speciation. Earth and Planetary Science Letters, 76, 263–278.

Flowers, G.C. (1979) Correction of Holloway's (1977) adaptation of the modified Redlich-Kwong equation of state for calculation of the fugacities of molecular species in supercritical fluids of geologic interest. Contributions to Mineralogy and Petrology, 69, 315–318.

Furukawa, T., Brawer, S.A., and White, W.B. (1978) Raman spectroscopic study of nitrate glasses. Journal of Chemical Physics, 69, 2639–2651.

Harris, D.M. (1981) The concentration of CO_2 in submarine tholeiitic basalts. Journal of Geology, 89, 689–701.

Holloway, J.R. (1977) Fugacity and activity of molecular species in supercritical fluids. In D. Fraser, Ed., Thermodynamics in geology, p. 161–181. D. Reidel, Boston, Massachusetts.

Johnson, T., Fine, G.J., and Stolper, E.M. (1985) Solubility of carbon dioxide in molten albite. EOS, 66, 1130.

Kennedy, G.C., Wasserburg, G.J., Heard, H.L., and Newton, R.C. (1962) The upper three phase region in the system SiO_2-H_2O. American Journal of Science, 260, 501–521.

Khitarov, N.I., and Kadik, A.A. (1973) Water and carbon dioxide in magmatic melts and peculiarities of the melting process. Contributions to Mineralogy and Petrology, 41, 205–215.

Kushiro, I. (1978) Viscosity and structural changes of albite ($NaAlSi_3O_8$) melt at high pressures. Earth and Planetary Science Letters, 41, 87–90.

Mathez, E.A. (1984) Influence of degassing on oxidation states of basaltic magmas. Nature, 310, 371–375.

Moore, J.G. (1979) Vesicularity and CO_2 in mid-ocean ridge basalt. Nature, 282, 250–253.

Mysen, B.O. (1976) The role of volatiles in silicate melts: Solubility of carbon dioxide and water in feldspar, pyroxene and feldspathoid melts to 30 kb and 1625 °C. American Journal of Science, 276, 969–996.

——— (1977) The solubility of H_2O and CO_2 under predicted magma genesis conditions and some petrological and geophysical implications. Reviews of Geophysics and Space Physics, 15, 351–361.

Mysen, B.O., and Virgo, D. (1980) The solubility behavior of CO_2 in melts on the join $NaAlSi_3O_8$-$CaAlSi_2O_6$-CO_2 at high pressures and temperatures: A Raman spectroscopic study. American Mineralogist, 65, 1166–1175.

Mysen, B.O., Eggler, D.H., Seitz, M.G., and Holloway, J.R. (1976) Carbon dioxide in silicate melts and crystals: Part I. Solubility measurements. American Journal of Science, 276, 455–479.

Nakamoto, K. (1978) Infrared and Raman spectra of inorganic and coordination compounds (third edition). Wiley, New York.

Pearce, M.L. (1964) Solubility of carbon dioxide and variation of oxygen ion activity in soda-silica melts. American Ceramic Society Journal, 47, 342–347.

Rai, C.S., Sharma, S.K., Meunow, D.W., Matson, D.W., and Byers, C.D. (1983) Temperature dependence of CO_2 solubility in high pressure quenched glasses of diopside composition. Geochimica et Cosmochimica Acta, 47, 953–958.

Seward, T.P., III. (1980) Coloration and optical anisotropy in silver-containing glasses. Journal of Non-Crystalline Solids, 40, 499–513.

Sharma, S.K. (1979) Structure and solubility of carbon dioxide in silicate glasses of diopside and sodium melilite compositions at high pressures from Raman spectroscopic data. Carnegie Institution of Washington Year Book 78, 532–537.

Silver, L.A., and Stolper, E. (1985) A thermodynamic model for hydrous silicate melts. Journal of Geology, 93, 161–178.

Spera, F.J., and Bergman, S.C. (1980) Carbon dioxide in igneous petrogenesis: I. Aspects of the dissolution of CO_2 in silicate liquids. Contributions to Mineralogy and Petrology, 74, 55–66.

Stolper, E. (1982a) Water in silicate glasses: An infrared spectroscopic study. Contributions to Mineralogy and Petrology, 81, 1–17.

——— (1982b) The speciation of water in silicate melts. Geochimica et Cosmochimica Acta, 46, 2609–2620.

Stolper, E., Silver, L.A., and Aines, R.D. (1983) The effects of quenching rate and temperature on the speciation of water in silicate glasses (abs.). EOS, 64, 339.

Watson, E.B., Sneeringer, M.A., and Ross, A. (1982) Diffusion of dissolved carbonate in magmas: Experimental results and applications. Earth and Planetary Science Letters, 61, 346–358.

Manuscript received November 25, 1985
Manuscript accepted July 2, 1987